




# Regional hyperperfusion in older adults with objectively-defined subtle cognitive decline

Kelsey R Thomas<sup>1,2</sup> , Jessica R Osuna<sup>1,2</sup>,  
Alexandra J Weigand<sup>1,2,3</sup>, Emily C Edmonds<sup>1,2</sup>,  
Alexandra L Clark<sup>1,2</sup>, Sophia Holmqvist<sup>1</sup>, Isabel H Cota<sup>1</sup>,  
Christina E Wierenga<sup>1,2</sup>, Mark W Bondi<sup>2,4</sup> and  
Katherine J Bangen<sup>1,2</sup>; for the Alzheimer's Disease  
Neuroimaging Initiative\*

## Abstract

Although cerebral blood flow (CBF) alterations are associated with Alzheimer's disease (AD), CBF patterns across prodromal stages of AD remain unclear. Therefore, we investigated patterns of regional CBF in 162 Alzheimer's Disease Neuroimaging Initiative participants characterized as cognitively unimpaired (CU;  $n = 80$ ), objectively-defined subtle cognitive decline (Obj-SCD;  $n = 31$ ), or mild cognitive impairment (MCI;  $n = 51$ ). Arterial spin labeling MRI quantified regional CBF in a priori regions of interest: hippocampus, inferior temporal gyrus, inferior parietal lobe, medial orbitofrontal cortex, and rostral middle frontal gyrus. Obj-SCD participants had increased hippocampal and inferior parietal CBF relative to CU and MCI participants and increased inferior temporal CBF relative to MCI participants. CU and MCI groups did not differ in hippocampal or inferior parietal CBF, but CU participants had increased inferior temporal CBF relative to MCI participants. There were no CBF group differences in the two frontal regions. Thus, we found an inverted-U pattern of CBF signal across prodromal AD stages in regions susceptible to early AD pathology. Hippocampal and inferior parietal hyperperfusion in Obj-SCD may reflect early neurovascular dysregulation, whereby higher CBF is needed to maintain cognitive functioning relative to MCI participants, yet is also reflective of early cognitive inefficiencies that distinguish Obj-SCD from CU participants.

## Keywords

Alzheimer's disease, cerebral blood flow, early detection, mild cognitive impairment, subtle cognitive decline

Received 20 December 2019; Revised 21 April 2020; Accepted 16 May 2020

## Introduction

Early detection of Alzheimer's disease (AD) in its pre-clinical phase has garnered significant attention in recent years, as this may be the optimal time to intervene to delay, slow, or prevent the onset of cognitive and functional impairment due to AD. Several studies have now shown that subtle cognitive changes can be captured in the preclinical phase of AD using sensitive neuropsychological measures and that these measures add prognostic value to predict future decline, above and beyond traditional AD biomarkers.<sup>1,2</sup> Neuropsychological process scores, for example, can be used to detect the cognitive inefficiencies associated

<sup>1</sup>Research Service, VA San Diego Healthcare System, San Diego, CA, USA

<sup>2</sup>Department of Psychiatry, University of California, San Diego, La Jolla, CA, USA

<sup>3</sup>San Diego State University/University of California, San Diego Joint Doctoral Program in Clinical Psychology, San Diego, CA, USA

<sup>4</sup>Psychology Service, VA San Diego Healthcare System, San Diego, CA, USA

\*Data used in preparation of this article were obtained from the Alzheimer's Disease Neuroimaging Initiative (ADNI) database (adni.loni.usc.edu). As such, the investigators within the ADNI contributed to the design and implementation of ADNI and/or provided data but did not participate in analysis or writing of this report. A complete listing of ADNI investigators can be found at: [http://adni.loni.usc.edu/wp-content/uploads/how\\_to\\_apply/ADNI\\_Acknowledgement\\_List.pdf](http://adni.loni.usc.edu/wp-content/uploads/how_to_apply/ADNI_Acknowledgement_List.pdf)

## Corresponding author:

Kelsey R Thomas, VA San Diego Healthcare System, 3350 La Jolla Village Drive, San Diego, CA 92161, USA.

Email: [kthomas@ucsd.edu](mailto:kthomas@ucsd.edu)

with AD, prior to the onset of dementia.<sup>2–6</sup> Process scores quantify the number and types of errors that an individual may make on a neuropsychological test or the approach and strategies that are used on a task.<sup>7</sup> These scores are distinct from the traditionally used overall total score and are often used to understand the cognitive profile of underlying brain pathology. Process scores derived from a word-list memory test, including intrusion errors, flattened learning slope, and susceptibility to retroactive interference have been shown to differ between cognitively unimpaired (CU) older adults who remain stably CU over five years relative to those who progress to mild cognitive impairment (MCI) or dementia within five years.<sup>2</sup>

Our recent work has integrated process scores into an existing definition of objectively-defined subtle cognitive decline (Obj-SCD) initially proposed by Edmonds et al.<sup>8,9</sup> Using these Edmonds/Thomas criteria, Obj-SCD is defined by performance > 1 standard deviation (SD) below the age-, education-, and sex-adjusted mean on: (1) two neuropsychological total scores in two different cognitive domains, (2) one neuropsychological total score and one process score, or (3) two process scores. Our work using this classification shows that Obj-SCD status predicts faster progression to MCI/dementia as well as more rapid functional decline, amyloid- $\beta$  (A $\beta$ ) accumulation, and entorhinal cortex atrophy relative to CU participants.<sup>9–11</sup> Additionally, Obj-SCD appears to have cross-sectional cerebrospinal fluid (CSF) and positron emission tomography (PET) AD biomarker abnormalities that fall in between CU and MCI participants,<sup>9,11</sup> providing further evidence that Obj-SCD can be identified coincident with accumulating amyloid and tau pathologies. However, we have not yet examined how Obj-SCD status relates to cerebrovascular pathology within individuals along the AD continuum.

The relationship between cerebrovascular pathology and AD has gained increasing attention in recent years, as evidence has emerged that vascular changes may accelerate cognitive changes associated with AD pathology, or, in fact, may be the part of the earliest phase of AD pathogenesis.<sup>12–15</sup> Cerebral blood flow (CBF) is critical for brain function, as it ensures adequate delivery of oxygen, glucose, and nutrients to the brain as well as the removal of carbon dioxide and cellular waste. The vascular two-hit hypotheses of AD pathogenesis suggest that cerebral hypoperfusion (i.e. “hit one”) precedes and initiates AD pathogenesis (“hit two”), which suggests that CBF perfusion patterns could be an early biomarker of AD.<sup>15</sup> CBF measures the rate of delivery of arterial blood to the capillary bed in the brain (quantified as milliliters of blood per grams of tissue per minute) and can be measured in vivo via arterial spin labeling (ASL) magnetic

resonance imaging (MRI).<sup>16</sup> ASL is a non-invasive MRI technique in which arterial water is magnetically labeled and used as an endogenous tracer to measure CBF. It has advantages over traditional blood oxygenation level dependent (BOLD) fMRI signal since it is a direct measure of blood flow and has the potential to more accurately capture the magnitude and location of neural function given that the signal is localized to the capillary bed.<sup>16</sup>

Alterations in resting CBF are associated with progression through the stages of the AD continuum, though the relationship between CBF and disease severity does not appear to be linear. Specifically, later stages of AD are associated with hypoperfusion, while the early stages show a more complex relationship of initial hyperperfusion in preclinical stages with transition to decline in CBF during MCI,<sup>17</sup> though it is important to consider that these findings are largely from cross-sectional studies. Consistent with this model of early hyperperfusion in those in the early preclinical stages of AD, followed by hypoperfusion during the MCI phase, the current study aimed to examine whether CBF across *a priori*-specified regions of interest known to be susceptible to AD pathology differed between CU, Obj-SCD, and MCI groups.

## Method

Data used in the preparation of this article were obtained from the Alzheimer’s Disease Neuroimaging Initiative (ADNI) database ([adni.loni.usc.edu](http://adni.loni.usc.edu)). The ADNI was launched in 2003 as a public-private partnership, led by Principal Investigator Michael W. Weiner, MD. The primary goal of ADNI has been to test whether serial MRI, PET, other biological markers, and clinical and neuropsychological assessment can be combined to measure the progression of MCI and early AD. For up-to-date information, see [www.adni-info.org](http://www.adni-info.org). This study was approved by the University of California, San Diego institutional review board and the ADNI study was approved by the institutional review boards at each of the participating institutions. Written informed consent was obtained from all participants or authorized representatives at each site. All procedures were in accordance with the ethical standards of the institutional and/or national research committee and with the 1975 Helsinki Declaration and its later amendments.

## Participants

Specific enrollment criteria for ADNI have been previously described in detail elsewhere.<sup>18</sup> Briefly, participants from ADNI were 55–90 years old, had  $\geq 6$  years of education or work-history

equivalent, were fluent in English or Spanish, had a Geriatric Depression Scale <6, had a Hachinski Ischemia Scale <5, adequate vision and hearing to perform neuropsychological tests, were in generally good health and without significant head trauma or neurologic disease, were stable on permitted medications, and had a reliable study partner. The current study included 162 participants from ADNI GO/ADNI 2 cohorts (when ASL MRI was collected); participants did not have dementia at their first study visit (classified as CU, as having a subjective memory complaint, early MCI, or late MCI by ADNI), had ASL data within 12 months of their baseline visit, and also had available baseline neuropsychological testing and [<sup>18</sup>F] fluorodeoxyglucose (FDG) PET imaging.

### Cognitive groups

First, Jak/Bondi actuarial neuropsychological MCI criteria were applied to all participants in this sample.<sup>19,20</sup> Relative to the conventional MCI criteria used in ADNI that rely heavily on a subjective clinical rating and a single memory test score and, as a result, show artificially low MCI-to-CU reversion rates,<sup>21</sup> this Jak/Bondi approach uses available objective neuropsychological test scores and has been shown to reduce the number of “false positive” diagnostic errors. Specifically, by using neuropsychological tests, this approach showed that approximately one-third of ADNI MCI participants exhibit biomarker profiles, neuropsychological performances, and functional trajectories that are more in-line with CU participants than MCI participants;<sup>20,22–24</sup> this Jak/Bondi approach also produced a realistic, yet slightly improved, MCI-to-CU reversion rate relative to the literature.<sup>25</sup> Using this method, participants were considered MCI if they performed >1 SD below the age-/education-/sex-adjusted mean on: (1) two neuropsychological measures within the same cognitive domain, or (2) at least one measure across all three sampled cognitive domains, or (3) a score of 6 or higher on the Functional Activities Questionnaire score.<sup>19,20</sup> Six neuropsychological test scores were considered in the Jak/Bondi diagnostic criteria for MCI, including two *memory* measures (Rey Auditory Verbal Learning Test (AVLT) delayed free recall correct responses and AVLT recognition (hits minus false positives)); two *language* measures (30-item Boston Naming Test (BNT) total correct and Animal Fluency total score), and two *attention/executive functioning* measures (Trail Making Test (TMT) Parts A and B times to completion).

Next, Edmonds/Thomas actuarial neuropsychological Obj-SCD criteria were applied to the remaining participants without MCI or dementia. Consistent

with our previous work, participants were considered to have Obj-SCD if they performed >1 SD below the age-/education-/sex-adjusted mean on (1) one impaired total test score in two different cognitive domains (memory, language, attention/executive), or (2) two impaired neuropsychological process scores from the AVLT, or (3) one impaired total test score and one impaired process score.<sup>9–11</sup> The total test scores were the six neuropsychological variables used for determining MCI classification. The three process scores for the Obj-SCD classification were derived from the AVLT, which is a 15-word learning and memory test that includes five learning trials (List A, Trials 1–5), an interference list trial (List B), a short delay free recall trial (List A, Trial 6), a long delay free recall trial (List A, Trial 7), and delayed recognition. The process scores used in the Obj-SCD criteria were *learning slope* ((List A Trial 5 – List A Trial 1)/5), *retroactive interference* (List A Trial 6/List A Trial 5), and *total intrusion errors* (total number of extra-list intrusion errors across all recall trials). These scores were previously shown to differ between CU ADNI participants who remained stable and those who progressed to MCI within five years.<sup>9</sup>

For both the neuropsychological total scores and process scores, the z-scores were derived based on a sample of CU participants in ADNI who did not progress to MCI for the duration of their study participation (i.e. “robust” controls;  $N=385$ ). Consistent with our prior work in ADNI,<sup>11,22,25</sup> within the robust control group, each neuropsychological score was regressed on age, education, and sex. Next, the resulting regression weights were used to compute a predicted score for each participant on each score. The z-scores were then calculated by subtracting the predicted score from each participant’s actual score and then dividing by the test-specific regression model’s standard error of the estimate.

### Arterial spin labeling and structural MRI

Detailed information describing the ASL and structural MRI data acquisition and processing is available online; all imaging data (e.g. ASL, structural MRI, FDG PET) used in this study were previously processed and downloaded from <http://adni.loni.usc.edu/>. All briefly, MR imaging was performed on a 3.0 Tesla scanner using a pulsed ASL method (QUIPS II with thin-slice T1 periodic saturation) with echo-planar imaging.<sup>26</sup> Scan parameters include inversion time for arterial spins (TI1) = 700 ms, total transit time of spins (TI2) = 1900 ms, tag thickness = 100 mm, tag to proximal slice gap = 25.4 mm, repetition time = 3400 ms, echo time = 12 ms, field of view = 256 mm, matrix = 64 × 64, slice thickness = 4 mm, number of



axial slices = 24, time lag between slices = 22.5 ms. ASL MRI processing was largely automated using a MATLAB pipeline and involved motion correction, aligning each ASL frame to the first frame using a rigid body transformation, and least squares fitting using SPM8 (<http://www.fil.ion.ucl.ac.uk/spm/>). Perfusion-weighted images were computed as the difference of the mean-tagged and mean-untagged ASL data and were intensity scaled to account for signal decay during acquisition and to generate intensities in meaningful physiological units. After geometric distortion correction using Insight Toolkit libraries,<sup>27</sup> ASL images were aligned to structural T1 images using FSL (<http://www.fmrib.ox.ac.uk/fsl/>). To minimize the effects of the lower perfusion in white matter on CBF estimates, a partial volume correction was performed that assumed that CBF in gray matter is 2.5 times greater than in white matter; SPM8 was used for tissue segmentation. The partial volume-corrected perfusion-weighted images were normalized by the reference image (i.e. an estimate of blood water magnetization) to convert the signal into physical units (mL/100 g tissue/min). ADNI quality control procedures to determine a global pass/fail rating were based on visual inspection of signal uniformity, geometrical distortions, gray matter contrast, and presence of large, disruptive artifacts. If a rating of "unusable" in any of these categories resulted in a global "fail" those data were excluded.

Structural MRI was acquired during the same session as the ASL scan. A T1-weighted 3D MPRAGE sequence was acquired with the following parameters: with field of view = 256 mm, repetition time = 2300 ms, echo time = 2.98 ms, flip angle = 9°, and resolution =  $1.1 \times 1.1 \times 1.2 \text{ mm}^3$ . FreeSurfer (version 4.5.0) was used to skull-strip, segment, and parcellate the structural scans. T2-weighted fluid-attenuated inversion recovery (FLAIR) scans were collected with the following parameters: field of view = 280 mm, field of view phase = 100.0%, slice thickness = 8.0 mm, TR = 20 ms, TE = 5 ms, flip angle = 40°.

FreeSurfer-derived anatomical regions of interest (ROIs) were applied and used to extract CBF estimates for each participant. The primary analyses examined the following five a priori ROIs: (1) hippocampus, (2) inferior parietal lobe (IPL), (3) inferior temporal gyrus (ITG), (4) medial orbitofrontal cortex (mOFC), and (5) rostral middle frontal gyrus (rMFG). These regions were chosen given prior work showing these regions were vulnerable to early AD-related changes,<sup>28</sup> showed associations between CBF and AD severity,<sup>29</sup> as well as to be consistent with prior CBF analyses conducted in ADNI.<sup>29,30</sup> Also consistent with other CBF work in ADNI,<sup>29,30</sup> CBF of the precentral gyrus was selected to serve as the control reference region as

it is not thought to be impacted in early AD, allowing for adjustment of expected individual differences in CBF that are likely not due to AD pathologies. Mean CBF corrected for partial volume effects was extracted for each of the ROIs and reference region for each hemisphere separately (hemisphere-specific analyses are included in Supplemental Materials). However, to reduce the number of comparisons and ensure reliability, averaged bilateral CBF estimates for each ROI were used as the outcome variables within the current study. Bilateral CBF estimates were calculated by averaging the mean CBF of each hemisphere, with each hemisphere's contribution to the average, weighted by the surface area of the ROI for that hemisphere. A similar approach was used to create a global CBF variable was created from all FreeSurfer derived gray-matter cortical and subcortical regions (excluding cerebellum); global CBF was calculated by averaging all regions with each region's contribution to the average weighted by its volume. An additional global CBF variable without the ROIs in this study was also derived to determine whether any group differences in global CBF were driven by inclusion of the five ROIs. If participants were missing baseline ASL but had ASL within the first year of their baseline visit, the first occasion of ASL data was used (84% of participants had the ASL and cognitive testing visits within 3 months of each other; median absolute time between visits = 0.96 months, mean = 2.16 months, SD = 3.12 months).

### Cerebral metabolism

Brain glucose metabolism was measured by FDG PET. Detailed information describing the FDG PET data acquisition, processing, and analysis is available online at <http://adni.loni.usc.edu/>. Briefly, FDG scanning began 30 min after intravenous injection of an approximately 5 mCi dose of tracer. PET images were spatially normalized to a Montreal Neurological Institute (MNI) PET template. Consistent with prior work in ADNI, a composite meta-ROI that is comprised of the standardized uptake value ratios (SUVs) of the left and right angular gyri, left and right middle/inferior temporal gyri, and bilateral posterior cingulate gyrus was used as the covariate in current analyses as a measure of global brain metabolism. These brain regions demonstrate metabolic changes in MCI and AD that are associated with cognitive performance.<sup>31,32</sup> The meta-ROI was intensity normalized by dividing by the mean for a pons and cerebellum reference region.<sup>32</sup> FDG PET was included as a covariate so that the CBF effects could be interpreted as independent of glucose metabolism.

### White matter hyperintensity volume

Detailed methods for WMH volumetric quantification have been previously described in detail.<sup>33–36</sup> WMH volume was calculated using a Bayesian approach to segmentation of the high resolution T1-weighted and FLAIR scans. Briefly, non-brain tissues were removed from T1-weighted and FLAIR images, the FLAIR image was spatially aligned to the T1-weighted image, and MRI field artifacts were removed. Prior to WMH calculation, images were warped to a standard template space. The likelihood of WMH was estimated from FLAIR signal characteristics, prior probability maps of WMH occurrence calculated from previously supervised segmentations of independent FLAIR images from more than 700 individuals, and tissue class constraints. Then the segmented WMH masks were back-transformed to native space for volume calculation. If a participant was missing baseline WMH data, the first visit with WMH data was used as long as it was within 12 months of their baseline visit.

### Additional covariates and descriptive variables

Apolipoprotein E (APOE)  $\epsilon 4$  carrier status was determined by the presence of at least one  $\epsilon 4$  allele and was included as a covariate to adjust for the known effect of a  $\epsilon 4$  allele on risk for AD and CBF. Pulse pressure (systolic – diastolic blood pressure) is a proxy measure for arterial stiffness and is thought to serve as an index of vascular aging. Higher pulse pressure is associated with increased cerebrospinal fluid (CSF) p-tau levels and progression to AD<sup>37,38</sup> and was included as a covariate to determine whether differences in regional CBF persist above and beyond general vascular risk. To further characterize the sample, CSF AD markers were examined in a subset of participants ( $n=143$ ) who underwent a lumbar puncture. AD CSF markers were processed using Elecsys<sup>®</sup> immunoassays; AD biomarker positivity was determined using the previously determined CSF p-tau/A $\beta$  ratio cut-score of  $>0.0251$  pg/ml, which was optimized for the ADNI sample.<sup>39</sup>

### Statistical analyses

Descriptive variables were analyzed using one-way analyses of variance (ANOVAs) for continuous variables and Chi-squared tests for categorical variables. Two ANCOVAs examined group differences in total gray matter volume and total WMH volume after adjusting for age, sex, APOE  $\epsilon 4$  status, pulse pressure, and total intracranial volume. WMH volume was log-transformed given the non-normal distribution. Two additional ANCOVAs examined group differences in global CBF (with and without the five ROIs

included in the global CBF variable) after adjusting for age, sex, APOE  $\epsilon 4$  status, pulse pressure, cerebral metabolism measured using FDG PET. A multivariate analysis of covariance (MANCOVA) was used to examine group differences between CU, Obj-SCD, and MCI participants in CBF of five a priori ROIs: hippocampus, IPL, ITG, mOFC, and rMFG. Age, sex, APOE  $\epsilon 4$  status, pulse pressure, FDG PET, and precentral gyrus CBF were adjusted for in the analysis to account for vascular and metabolic factors that could influence CBF. Precentral gyrus CBF was used as a reference region due to its relative sparing from AD-related changes and its prior use for these purposes in ADNI CBF data.<sup>29,30</sup> The five ROIs were entered into the MANCOVA simultaneously, and follow-up least significant difference pairwise comparisons were restricted to those regions for which the MANOVA was significant. Statistical significance of the pairwise comparisons was also examined using false discovery rates (FDR) of 0.10 and 0.05.<sup>40</sup> To further explore whether the pattern of findings was retained in those who were p-tau/A $\beta$  positive (on the AD continuum), the ROI analyses were first repeated in the subset of participants considered p-tau/A $\beta$  positive and then only in those considered p-tau/A $\beta$  negative.

### Results

Participant characteristics by cognitive group are presented in Table 1. Regarding demographic variables, the Obj-SCD group was about three years older than the CU group, but not different from the MCI group. There were no differences in education level or sex by cognitive group. Participants with MCI were more likely to be APOE  $\epsilon 4$  carriers, have higher rates of CSF p-tau/A $\beta$  positivity, and lower FDG PET SUVR than CU participants, but only differed from Obj-SCD on FDG PET (with lower values). Obj-SCD had higher rates of CSF p-tau/A $\beta$  positivity than CU participants. As expected, across almost all neuropsychological measures, the MCI group performed the worst, followed by Obj-SCD, and then CU participants. There were no differences in time between ASL and cognitive testing visit by group.

The ANCOVA examining group differences in total gray matter, after adjusting for age, sex, APOE  $\epsilon 4$  status, pulse pressure, and total intracranial volume were significant [ $F(2,154)=4.01$ ,  $p=.020$ ,  $\eta_p^2=.049$ ] such that the CU group had greater total gray matter volume than the MCI group ( $p=.005$ ) but did not differ from the Obj-SCD group ( $p=.270$ ). The Obj-SCD and MCI groups did not differ from each other ( $p=.222$ ). There was one outlier in the MCI group with very high gray matter volume, so the model was also run without that participant and the pattern of results

**Table 1.** Descriptive variables by cognitive group.

|                                  | CU<br>(N = 80)                | Obj-SCD<br>(N = 31)           | MCI<br>(N = 51)               | F or $\chi^2$    | $\eta_p^2$ or $\Phi$ | p     |
|----------------------------------|-------------------------------|-------------------------------|-------------------------------|------------------|----------------------|-------|
| Age                              | 70.12 (5.88) <sup>b</sup>     | 73.14 (7.07) <sup>c</sup>     | 71.91 (7.34)                  | F = 2.54         | $\eta_p^2 = .031$    | .082  |
| Education                        | 16.69 (2.68)                  | 16.68 (2.12)                  | 16.35 (2.73)                  | F = 0.28         | $\eta_p^2 = .004$    | .753  |
| Female, % (n)                    | 53.8% (n = 43)                | 51.6% (n = 16)                | 41.2% (n = 21)                | $\chi^2 = 2.05$  | $\Phi = .112$        | .359  |
| Pulse pressure/                  | 59.70 (14.24)                 | 62.55 (17.10)                 | 56.94 (17.36)                 | F = 1.24         | $\eta_p^2 = .015$    | .291  |
| APOE $\epsilon 4$ carrier, % (n) | 33.8% (n = 27) <sup>a</sup>   | 35.5% (n = 11)                | 52.9% (n = 27) <sup>c</sup>   | $\chi^2 = 5.12$  | $\Phi = .178$        | .077  |
| CSF p-tau/A $\beta$ positive*    | 18.6% (n = 13) <sup>a,b</sup> | 42.3% (n = 11) <sup>a,c</sup> | 68.1% (n = 32) <sup>b,c</sup> | $\chi^2 = 29.07$ | $\Phi = .451$        | <.001 |
| FDG-PET SUVR                     | 1.31 (0.12) <sup>a</sup>      | 1.29 (0.11) <sup>a</sup>      | 1.21 (0.13) <sup>b,c</sup>    | F = 11.05        | $\eta_p^2 = .122$    | <.001 |
| MMSE                             | 29.06 (1.12) <sup>a</sup>     | 29.03 (1.25) <sup>a</sup>     | 27.67 (1.88) <sup>b,c</sup>   | F = 16.56        | $\eta_p^2 = .172$    | <.001 |
| Animal fluency                   | 23.45 (5.12) <sup>a,b</sup>   | 18.84 (5.07) <sup>c</sup>     | 16.98 (5.16) <sup>c</sup>     | F = 26.95        | $\eta_p^2 = .253$    | <.001 |
| BNT (30 item)                    | 28.54 (1.54) <sup>a</sup>     | 27.71 (2.56) <sup>a</sup>     | 26.18 (3.86) <sup>b,c</sup>   | F = 12.25        | $\eta_p^2 = .134$    | <.001 |
| Trails A                         | 27.73 (6.79) <sup>a,b</sup>   | 36.67 (10.68) <sup>a,c</sup>  | 42.90 (17.77) <sup>b,c</sup>  | F = 25.77        | $\eta_p^2 = .245$    | <.001 |
| Trails B                         | 71.38 (26.74) <sup>a</sup>    | 86.37 (25.24) <sup>a</sup>    | 118.90 (76.82) <sup>b,c</sup> | F = 14.76        | $\eta_p^2 = .160$    | <.001 |
| AVLT delayed recall              | 9.86 (3.57) <sup>a,b</sup>    | 5.29 (3.62) <sup>a,c</sup>    | 2.82 (3.01) <sup>b,c</sup>    | F = 69.73        | $\eta_p^2 = .467$    | <.001 |
| AVLT recognition                 | 28.28 (1.54) <sup>a,b</sup>   | 25.87 (2.49) <sup>a,c</sup>   | 22.67 (3.61) <sup>b,c</sup>   | F = 76.41        | $\eta_p^2 = .490$    | <.001 |
| AVLT learning slope              | 1.32 (0.44) <sup>a,b</sup>    | 0.90 (0.47) <sup>c</sup>      | 0.77 (0.47) <sup>c</sup>      | F = 24.48        | $\eta_p^2 = .235$    | <.001 |
| AVLT retroactive interference    | 0.85 (0.14) <sup>a,b</sup>    | 0.64 (0.33) <sup>c</sup>      | 0.54 (0.32) <sup>c</sup>      | F = 25.28        | $\eta_p^2 = .241$    | <.001 |
| AVLT intrusion errors            | 3.36 (4.17) <sup>b</sup>      | 5.45 (4.24) <sup>c</sup>      | 4.12 (3.36)                   | F = 3.16         | $\eta_p^2 = .038$    | .045  |

CU: cognitively unimpaired; Obj-SCD: objectively-defined subtle cognitive decline; MCI: mild cognitive impairment; CSF: cerebrospinal fluid; FDG-PET: fluorodeoxyglucose-PET; SUVR: standardized uptake value ratio; CBF: cerebral blood flow; MMSE: mini mental state exam; BNT: Boston Naming Test; AVLT: Rey Auditory Verbal Learning Test.

<sup>a</sup>Significantly different from MCI group ( $p < .05$ ).

<sup>b</sup>Significantly different from Obj-SCD group.

<sup>c</sup>Significantly different from CU group.

\*Subsample of 70 CU, 26 Obj-SCD, 47 MCI with CSF data.

did not change. There were also group differences in total WMH volume [ $F(2,154) = 3.77$ ,  $p = .025$ ,  $\eta_p^2 = .047$ ] such that the CU group had lower WMH volume than the MCI group ( $p = .008$ ) but did not differ from the Obj-SCD group ( $p = .178$ ). The Obj-SCD and MCI groups did not differ from each other ( $p = .370$ ). The ANCOVA examining differences in global CBF, after adjusting for age, sex, APOE  $\epsilon 4$  status, pulse pressure, and FDG PET were significant [ $F(2,148) = 5.02$ ,  $p = .008$ ,  $\eta_p^2 = .064$ ] such that the MCI group had hypoperfusion relative to the CU ( $p = .004$ ) and Obj-SCD ( $p = .011$ ) groups. The CU and Obj-SCD did not differ from each other ( $p > .05$ ). There was one outlier in the Obj-SCD group, but the results did not change when that participant was removed from analyses. Another ANCOVA was run examining group differences in a global CBF variable that did not include the five a priori ROIs; however, when the five ROIs were removed from the global CBF, there was no longer an effect of group on global CBF ( $p > .05$ ). The significant group differences were retained under both a 0.10 FDR and 0.05 FDR. Figure 1 shows the gray matter volumes, WMH volumes, and global CBF (that includes the ROIs) of each group.

The MANCOVA omnibus test indicated a significant effect of cognitive group on CBF [ $F(10, 300) = 2.04$ ,  $p = .029$ ,  $\eta_p^2 = .064$ ]. Specifically, there was a

significant effect of cognitive group on three CBF ROIs, including the hippocampus [ $F(2,153) = 4.20$ ,  $p = .017$ ,  $\eta_p^2 = .052$ ], IPL [ $F(2,153) = 3.07$ ,  $p = .049$ ,  $\eta_p^2 = .039$ ], and ITG [ $F(2,153) = 5.56$ ,  $p = .005$ ,  $\eta_p^2 = .068$ ]. The mOFC and rMFG ROIs were not significant ( $ps > .05$ ), and therefore the post hoc analyses were not examined. Figure 2 shows the CBF of each group by ROI. Post hoc analyses showed that hippocampal CBF was higher in Obj-SCD than CU ( $p = .007$ ) and MCI participants ( $p = .016$ ), but CU and MCI groups did not differ ( $p = .974$ ). A similar pattern was found for the IPC such that Obj-SCD showed hyperperfusion relative to the CU ( $p = .040$ ) and MCI groups ( $p = .020$ ), but the CU and MCI groups did not differ ( $p = .550$ ). For the ITG, Obj-SCD had higher CBF than the MCI group ( $p = .002$ ), but did not differ from the CU group ( $p = .274$ ). The CU group also had higher ITG CBF than the MCI group ( $p = .010$ ). The significant hippocampus and ITG CBF group differences were retained under both a 0.10 FDR and 0.05 FDR. The significant IPL results were retained under a 0.10 FDR, but not a 0.05 FDR. One participant in the CU group was considered an outlier; however, the pattern of results did not change when they were excluded. Hemisphere-specific analyses are included in Supplemental Materials; the pattern of results was largely identical with group differences in

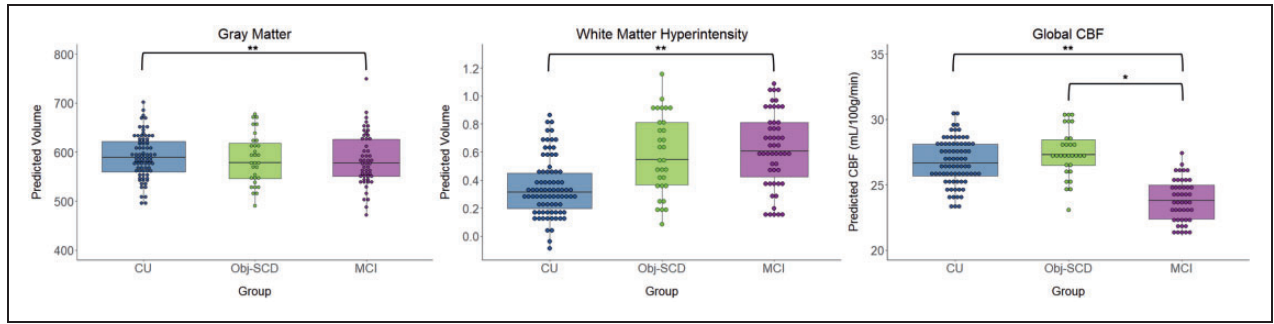


**Figure 1.** Gray matter volume, white matter hyperintensity volume, and global CBF by cognitive group. \* $p < .05$ , \*\* $p < .01$ ; White matter hyperintensity volume was log-transformed; Model predicted volumes for gray matter and white matter hyperintensities were adjusted for age, sex, APOE  $\epsilon 4$  status, pulse pressure, and total intracranial volume; global CBF was adjusted for age, sex, APOE  $\epsilon 4$  status, pulse pressure, and FDG PET. CU: cognitively unimpaired; Obj-SCD: objectively-defined subtle cognitive decline; MCI: mild cognitive impairment.

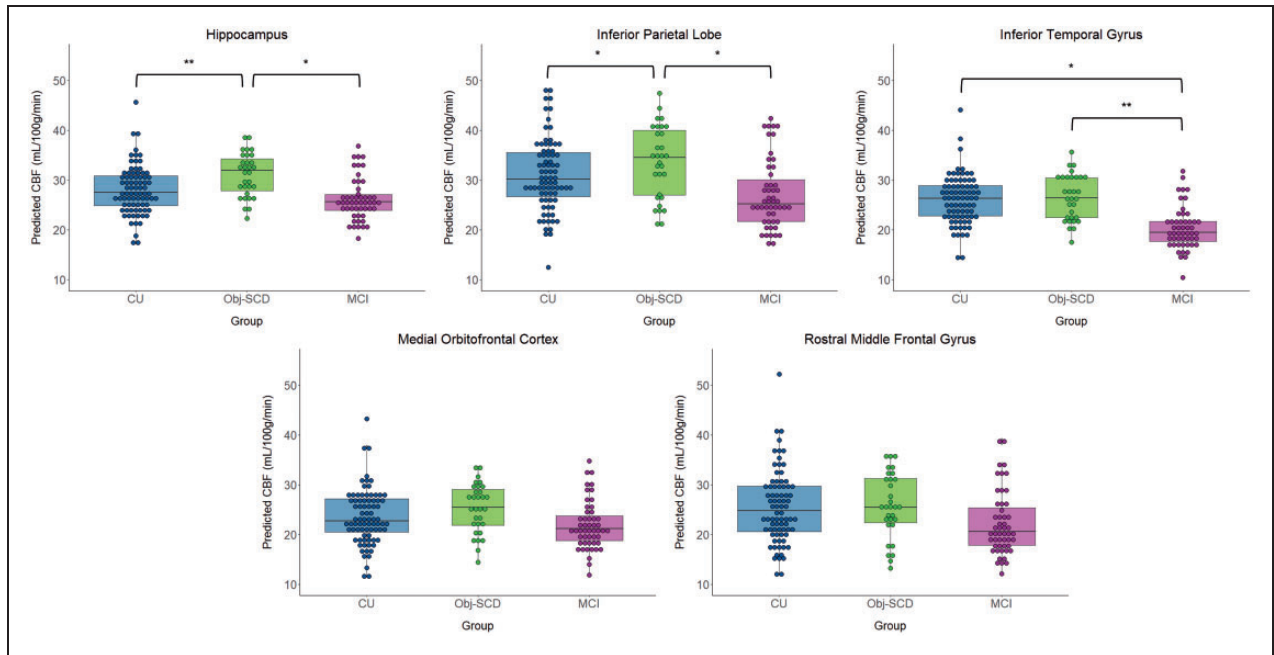


**Figure 2.** CBF by cognitive group across the five a priori regions of interest. \* $p < .05$ , \*\* $p < .01$ . Model predicted CBF was adjusted for age, sex, APOE  $\epsilon 4$  status, pulse pressure, FDG PET, and precentral gyrus CBF. CBF: cerebral blood flow; CU: cognitively unimpaired; Obj-SCD: objectively-defined subtle cognitive decline; MCI: mild cognitive impairment.

left and right hippocampus and ITG, though the left and right IPL region results were slightly attenuated when they were examined separately instead of averaged across hemispheres.

Finally, exploratory sensitivity analyses were conducted to examine whether the pattern of regional hyperperfusion in the Obj-SCD group retained when only those who were considered p-tau/A $\beta$  positive were included in analyses; then the analyses were repeated in participants who were considered p-tau/A $\beta$  negative. In p-tau/A $\beta$  positive participants (CU

$n = 13$ , Obj-SCD  $n = 11$ , MCI  $n = 32$ ), there was a significant effect of group on hippocampal CBF [ $F(2,47) = 3.55$ ,  $p = .037$ ,  $\eta_p^2 = .131$ ] and rMFG CBF [ $F(2,47) = 4.75$ ,  $p = .013$ ,  $\eta_p^2 = .168$ ], and similar, though attenuated, pattern for ITG [ $F(2,47) = 3.15$ ,  $p = .052$ ,  $\eta_p^2 = .118$ ] and IPL [ $F(2,47) = 2.07$ ,  $p = .137$ ,  $\eta_p^2 = .081$ ]. There was not a significant effect of group on mOFC CBF. Pairwise comparisons are shown in Supplementary Material, but across the hippocampus, rMFG, and ITG, the Obj-SCD group had hyperperfusion relative to the CU and MCI groups ( $ps < .05$ ), and



the CU and MCI groups not differ from each other. The IPL group comparisons had a similar pattern, but was at trend level ( $ps < .1$ ). When these analyses were explored in p-tau/A $\beta$  negative participants (CU  $n = 57$ , Obj-SCD  $n = 15$ , MCI  $n = 15$ ), there was not a significant effect of group on any of the CBF ROIs ( $ps > .05$ ).

## Discussion

The current study found an inverted-U pattern of CBF across the stages of prodromal AD in key ROIs that are susceptible to early AD pathology. Specifically, the Obj-SCD group showed increased CBF in the hippocampus, IPL, and ITG relative to the MCI group and increased CBF in the hippocampus and IPL relative to the CU group. There were no differences in CBF across frontal regions in the primary analyses. Our study extends prior work that has investigated biomarker associations with the Obj-SCD classification by examining very early neurovascular changes in regions susceptible to AD pathology, and further demonstrates the utility of ASL MRI as a biomarker of early AD-related changes.

Our findings are consistent with prior work that has found higher regional CBF in participants at risk for progression to AD, but who are not yet considered cognitively impaired.<sup>41,42</sup> For example, CU participants who were APOE  $\epsilon 4$  carriers have shown increased medial temporal CBF relative to non-carriers.<sup>42,43</sup> Other studies have examined CBF in CU individuals at elevated risk for AD, including individuals who are A $\beta$  positive on PET imaging,<sup>12</sup> APOE  $\epsilon 4$  carriers,<sup>44,45</sup> or those with self-reported cognitive decline.<sup>46</sup> These studies have demonstrated a negative relationship between cognition and CBF in the at-risk group, but a positive relationship or no significant relationship between cognition and CBF in the group without the AD risk factor. This is consistent with the observed pattern in which the Obj-SCD group performed worse on cognitive measures than the CU group but showed regional hyperperfusion relative to the CU group. One possible explanation for this consistent pattern across unimpaired participants at high risk for progression to MCI or dementia, including Obj-SCD, is that higher CBF may indicate a vascular compensatory response to very early pathologic processes, whereby higher CBF is needed to maintain intact cognitive functioning relative to the MCI group, yet is also reflective of the increased errors and inefficiencies in performance that distinguish the Obj-SCD from CU group.

The mechanisms behind this complex relationship of hyperperfusion in CU participants at higher risk for AD are not fully understood. However, Østergaard and colleagues<sup>47</sup> capillary dysfunction hypothesis

suggests that increased heterogeneity of capillary blood flow patterns may occur early in preclinical AD and require increased CBF to maintain sufficient brain oxygenation. As the disease progresses, continued increases in capillary blood flow heterogeneity may subsequently result in low tissue oxygen that require neurovascular adjustments such as suppression of CBF to maintain tissue metabolism. Therefore, early regional compensatory hyperperfusion, such as that observed in the Obj-SCD group, and later hypoperfusion known to occur in later MCI and AD stages, fits within this hypothesis.<sup>17,29,30,43</sup> This pattern is also consistent with what was observed for the pattern of global CBF, in that the early hyperperfusion of the Obj-SCD group appears to be region-specific, rather than a global pattern, and that global hypoperfusion is evident at the MCI stage.

While there was a qualitative pattern of higher CBF across all five a priori regions, the inverted-U pattern across the CU, Obj-SCD, and MCI groups was most salient for the hippocampus and inferior parietal lobe. This pattern was not observed in the global CBF analysis in which the CU and Obj-SCD groups did not differ, while the MCI group had reduced global CBF. Given that the Obj-SCD group showed higher rates of CSF p-tau/A $\beta$  positivity, it is possible that early AD pathology in the medial temporal lobe is causing the need for hyperperfusion of the hippocampus in order to maintain sufficient brain oxygenation. Results of the sensitivity analyses are consistent with this hypothesis since the pattern of regional hyperperfusion was retained when analyses were run only in those with an elevated CSF p-tau/A $\beta$  ratio (considered to be on the AD continuum), but was not present when analyses were run only in those who were p-tau/A $\beta$  negative. However, these results should be interpreted with caution given the extremely small group sizes and cross-sectional nature. Postmortem studies of individuals with asymptomatic (i.e. preclinical) AD have demonstrated this similar inverted-U pattern in cortical neuron and nuclei volume. In these studies, the preclinical AD group showed hypertrophy of cortical neurons and their nuclei in AD vulnerable regions, including in the CA1 region of the hippocampus, relative to both normal control and MCI participants.<sup>48,49</sup> This work suggested that the hypertrophy of cortical neurons and their nuclei in the preclinical AD participants may either represent an early response to toxic A $\beta$  and tau proteins or is a protective response that allows individuals with AD pathology to compensate in order to maintain normal cognition. The hypertrophied neurons/nuclei may, in turn, require increased blood flow to maintain neuronal health and functionality.

Conversely, since Obj-SCD has been shown to be associated with future amyloid accumulation and



neurodegeneration,<sup>11</sup> it is possible that early neurovascular dysfunction occurs very early and results in the subsequent accumulation of A $\beta$  and tau. This latter hypothesis would be consistent with Zlokovic's two-hit hypothesis of AD pathogenesis<sup>15</sup> in which primary microvascular damage ("hit one") initiates vascular-mediated neuronal dysfunction, such as blood-brain barrier dysfunction, neurotoxic secretion, and micro-ischemic events. Next, the blood-brain barrier dysfunction and ischemia result in impaired clearance of and subsequent accumulation of amyloid- $\beta$  ("hit two").<sup>50</sup> Although "hit one" is generally thought to describe hypoperfusion rather than hyperperfusion, the two-hit hypothesis may fit best in the context of more progressed prodromal AD (e.g. MCI), while Østergaard's capillary dysfunction hypothesis suggesting increased CBF to maintain brain oxygenation may be more in line with the very early preclinical stage that Obj-SCD captured.

Beyond amyloid and tau pathology, it is possible that the hyperperfusion of the inferior parietal lobe in the Obj-SCD group may be associated with or predictive of early white matter disease. WMHs have been shown to be important for predicting progression to MCI and AD.<sup>51,52</sup> Furthermore, work from the Dominantly Inherited Alzheimer Network (DIAN) study, which included presymptomatic carriers of a deterministic gene mutation for AD (PSEN1, PSEN2, APP) and non-carrier first-degree relatives, showed that WMHs may be a core pathology associated with AD. Specifically, parietal and occipital lobe WMH volume was higher in mutation carriers approximately 22 years prior to estimated symptom onset.<sup>14</sup> Thus, the inferior parietal hyperperfusion in the Obj-SCD may be associated with the very early posterior cerebrovascular changes associated with preclinical AD. We examined whether there were group differences in total WMH volume by group and found that the MCI group had greater WMH volume than the CU group. Although the Obj-SCD group did not significantly differ from the CU group, their mean WMH volume was much closer to the MCI groups' than the CU group (see Figure 1). This pattern may suggest that there is a relationship between the need for increased CBF in Obj-SCD participants that may ultimately precede the downstream structural changes of increased WMH volume. Regional WMH volume was not available for the current study, but future research should examine the longitudinal relationships between CBF and regional WMH volume across the AD clinical continuum, including among those with Obj-SCD.

The current study is limited by the small sample size, particularly in the Obj-SCD group, and the cross-sectional design precludes conclusions about causation despite interpretation that findings represent

differences along the AD continuum. Future work that integrates longitudinal CBF, AD biomarkers (e.g., amyloid and tau PET), and cognition data would help to disentangle these complex, and potentially causal relationships. Additionally, multiple analyses were conducted, though we used a MANCOVA (rather than multiple univariate analyses) and only examined the post hoc comparisons for ROIs that were significant. This approach was modeled from a previously published three-group (A $\beta$ +, A $\beta$ -, and AD) study that used CBF data from ADNI.<sup>29</sup> Our pattern of results was retained when an FDR of 0.10 was used, and all results except for the IPL post hoc pattern of significance were retained using an FDR of 0.05. Bilateral ROIs were also created to reduce comparisons, particularly given the relative consistency of findings across hemispheres. Our study is also limited in its generalizability beyond this mostly white, highly educated, and very healthy ADNI sample. It is very possible that results may change in populations with higher rates of vascular diseases. However, it is noteworthy that we were able to detect CBF difference despite ADNI participants being such a healthy sample (all Hachinski scores < 5). Although the most common underlying neurodegenerative process in these Obj-SCD and MCI groups is likely AD, the current study did not include autopsy-based pathological confirmation, and therefore cannot rule out the possibility that non-AD pathologies could also be contributing to these cognitive and CBF differences. Strengths of the current study include the ability to characterize and adjust for vascular and metabolic markers that could impact CBF as well as examine other variables such as total WMH volume to better understand the possible mechanisms and implications for the group differences in CBF. The current study also adjusted for APOE  $\epsilon$ 4 carrier status. Thus, the finding that CBF group differences, particularly in hippocampal and inferior parietal regions, persisted after these adjustments suggests relatively robust effects and that CBF is an independent contributor/risk factor rather than a byproduct of other risk factors.

Taken together, our findings add to the expanding literature to suggest that the Edmonds/Thomas actuarial Obj-SCD definition, which includes both neuropsychological total scores and process scores, is a sensitive and accessible marker of individuals at elevated risk for future progression to MCI/dementia as well as future functional difficulties, amyloid accumulation, and medial temporal neurodegeneration.<sup>9-11</sup> The consistent findings of associations between the Obj-SCD criteria and both clinical progression and sensitive AD biomarkers provide further support for the use of these criteria in clinical research to better capture the subtle cognitive changes that occur very early in the

preclinical stage of AD. The findings of increased hippocampal and inferior parietal CBF in the Obj-SCD group relative to the CU and MCI groups suggest that hyperperfusion of these regions may be an early biological marker of cognitive inefficiency due to AD.

### Funding

The author(s) disclosed receipt of the following financial support for the research, authorship, and/or publication of this article: This work was supported by the U.S. Department of Veterans Affairs Clinical Sciences Research and Development Service (Career Development Award-2 1IK2CX001865 to K. R.T., 1IK2CX000938 to K.J.B., and 1IK2CX001415 to E.C.E.; Merit Award 1I01CX001842 to K.J.B and 5I01CX000565 to C.E.W.), NIH grants (R01 AG049810 and R01 AG054049 to M.W.B.), and the Alzheimer's Association (AARF-17-528918 to K.R.T., AARG-18-566254 to K.J.B., AARG-17-500358 to E.C.E.). Data collection and sharing for this project were funded by the Alzheimer's Disease Neuroimaging Initiative (ADNI) (National Institutes of Health Grant U01 AG024904) and DOD ADNI (Department of Defense award number W81XWH-12-2-0012). ADNI is funded by the National Institute on Aging, the National Institute of Biomedical Imaging and Bioengineering, and through generous contributions from the following: AbbVie, Alzheimer's Association; Alzheimer's Drug Discovery Foundation; Araclon Biotech; BioClinica, Inc.; Biogen; Bristol-Myers Squibb Company; CereSpir, Inc.; Cogstate; Eisai Inc.; Elan Pharmaceuticals, Inc.; Eli Lilly and Company; EuroImmun; F. Hoffmann-La Roche Ltd and its affiliated company Genentech, Inc.; Fujirebio; GE Healthcare; IXICO Ltd.; Janssen Alzheimer Immunotherapy Research & Development, LLC.; Johnson & Johnson Pharmaceutical Research & Development LLC.; Lumosity; Lundbeck; Merck & Co., Inc.; Meso Scale Diagnostics, LLC.; NeuroRx Research; Neurotrack Technologies; Novartis Pharmaceuticals Corporation; Pfizer Inc.; Piramal Imaging; Servier; Takeda Pharmaceutical Company; and Transition Therapeutics. The Canadian Institutes of Health Research is providing funds to support ADNI clinical sites in Canada. Private sector contributions are facilitated by the Foundation for the National Institutes of Health ([www.fnih.org](http://www.fnih.org)). The grantee organization is the Northern California Institute for Research and Education, and the study is coordinated by the Alzheimer's Therapeutic Research Institute at the University of Southern California. ADNI data are disseminated by the Laboratory for Neuro Imaging at the University of Southern California.

### Declaration of conflicting interests

The author(s) declared the following potential conflicts of interest with respect to the research, authorship, and/or publication of this article: Dr. Bondi receives royalties from

Oxford University Press and serves as a consultant for Eisai, Novartis, and Roche Pharmaceutical. Other authors report no disclosures.

### Authors' contributions

Dr. Thomas designed and conceptualized the study, obtained, analyzed, and interpreted the data, and drafted the manuscript.

Ms. Osuna obtained and analyzed the data and revised the manuscript for intellectual content.

Ms. Weigand obtained and interpreted the data and revised the manuscript for intellectual content.

Dr. Edmonds obtained and interpreted the data and revised the manuscript for intellectual content.

Dr. Clark interpreted the data and revised the manuscript for intellectual content.

Ms. Holmqvist interpreted the data and revised the manuscript for intellectual content.

Ms. Cota interpreted the data and revised the manuscript for intellectual content.

Dr. Wierenga interpreted the data and revised the manuscript for intellectual content.

Dr. Bondi obtained and interpreted the data and revised the manuscript for intellectual content.

Dr. Bangen designed and conceptualized the study, obtained, analyzed, and interpreted the data, and drafted the manuscript.

### ORCID iD

Kelsey R Thomas  <https://orcid.org/0000-0003-4277-8876>

### Supplementary material

Supplemental material for this article is available online.

### References

- Jedynak BM, Lang A, Liu B, et al. A computational neurodegenerative disease progression score: method and results with the Alzheimer's disease neuroimaging initiative cohort. *Neuroimage* 2012; 63: 1478–1486.
- Thomas KR, Eppig J, Edmonds EC, et al. Word-list intrusion errors predict progression to mild cognitive impairment. *Neuropsychology* 2018; 32: 235–245.
- Abulafia C, Loewenstein D, Curiel-Cid R, et al. Brain structural and amyloid correlates of recovery from semantic interference in cognitively normal individuals with or without family history of late-onset Alzheimer's disease. *J Neuropsychiatry Clin Neurosci* 2018; 31: 25–36.
- Libon DJ, Bondi MW, Price CC, et al. Verbal serial list learning in mild cognitive impairment: a profile analysis of interference, forgetting, and errors. *J Int Neuropsychol Soc* 2011; 17: 905–914.
- Loewenstein DA, Curiel RE, DeKosky S, et al. Utilizing semantic intrusions to identify amyloid positivity in mild cognitive impairment. *Neurology* 2018; 91: e976–e984.

6. Loewenstein DA, Curiel RE, Duara R, et al. Novel cognitive paradigms for the detection of memory impairment in pre-clinical Alzheimer's disease. *Assessment* 2018; 25: 348–359.
7. Kaplan, E. A process approach to neuropsychological assessment. In: T. Boll & B. K. Bryant (eds) *Clinical neuropsychology and brain function: Research, measurement, and practice*. Washington DC: American Psychological Association, 1988, pp. 127–167.
8. Edmonds EC, Delano-Wood L, Galasko DR, et al. Subtle cognitive decline and biomarker staging in preclinical Alzheimer's disease. *J Alzheimers Dis* 2015; 47: 231–242.
9. Thomas KR, Edmonds EC, Eppig J, et al. Using neuropsychological process scores to identify subtle cognitive decline and predict progression to mild cognitive impairment. *J Alzheimers Dis* 2018; 64: 195–204.
10. Thomas KR, Bangen KJ, Weigand AJ, et al. Type II diabetes interacts with Alzheimer disease risk factors to predict functional decline. *Alzheimer Dis Assoc Disord* 2020; 34: 10–17.
11. Thomas KR, Bangen KJ, Weigand AJ, et al. Objective subtle cognitive difficulties predict future amyloid accumulation and neurodegeneration. *Neurology* 2020; 94: e397–e406.
12. Bangen KJ, Clark AL, Edmonds EC, et al. Cerebral blood flow and amyloid- $\beta$  interact to affect memory performance in cognitively normal older adults. *Front Aging Neurosci* 2017; 9: 181.
13. Bangen KJ, Nation DA, Delano-Wood L, et al. Aggregate effects of vascular risk factors on cerebrovascular changes in autopsy-confirmed Alzheimer's disease. *Alzheimers Dement* 2015; 11: 394–403.e1.
14. Lee S, Viqar F, Zimmerman ME, et al. White matter hyperintensities are a core feature of Alzheimer's disease: evidence from the dominantly inherited Alzheimer network. *Ann Neurol* 2016; 79: 929–939.
15. Zlokovic BV. Neurovascular pathways to neurodegeneration in Alzheimer's disease and other disorders. *Nat Rev Neurosci* 2011; 12: 723–738.
16. Liu TT and Brown GG. Measurement of cerebral perfusion with arterial spin labeling: part 1. Methods. *J Int Neuropsychol Soc* 2007; 13: 517–525.
17. Wierenga CE, Hays CC and Zlatar ZZ. Cerebral blood flow measured by arterial spin labeling MRI as a preclinical marker of Alzheimer's disease. *J Alzheimers Dis* 2014; 42: S411–S419.
18. Petersen RC, Aisen PS, Beckett LA, et al. Alzheimer's disease neuroimaging initiative (ADNI): clinical characterization. *Neurology* 2010; 74: 201–209.
19. Jak AJ, Bondi MW, Delano-Wood L, et al. Quantification of five neuropsychological approaches to defining mild cognitive impairment. *Am J Geriatr Psychiatry* 2009; 17: 368–375.
20. Bondi MW, Edmonds EC, Jak AJ, et al. Neuropsychological criteria for mild cognitive impairment improves diagnostic precision, biomarker associations, and progression rates. *J Alzheimers Dis* 2014; 42: 275–289.
21. Thomas KR, Eppig JS, Weigand AJ, et al. Artificially low mild cognitive impairment to normal reversion rate in the Alzheimer's disease neuroimaging initiative. *Alzheimers Dement* 2019; 15: 561–569.
22. Edmonds EC, Delano-Wood L, Clark LR, et al. Susceptibility of the conventional criteria for mild cognitive impairment to false-positive diagnostic errors. *Alzheimers Dement* 2015; 11: 415–424.
23. Thomas KR, Edmonds EC, Delano-Wood L, et al. Longitudinal trajectories of informant-reported daily functioning in empirically defined subtypes of mild cognitive impairment. *J Int Neuropsychol Soc* 2017; 23: 521–527.
24. Bangen KJ, Clark AL, Werhane M, et al. Cortical amyloid burden differences across empirically-derived mild cognitive impairment subtypes and interaction with APOE  $\epsilon$ 4 genotype. *J Alzheimers Dis* 2016; 52: 849–861.
25. Thomas KR, Edmonds EC, Eppig JS, et al. MCI-to-normal reversion using neuropsychological criteria in the Alzheimer's disease neuroimaging initiative. *Alzheimers Dement* 2019; 15: 1322–1332.
26. Luh W-M, Wong EC, Bandettini PA, et al. QUIPSS II with thin-slice T1I periodic saturation: a method for improving accuracy of quantitative perfusion imaging using pulsed arterial spin labeling. *Magn Reson Med* 1999; 41: 1246–1254.
27. Yoo TS, Ackerman MJ, Lorensen WE, et al. Engineering and algorithm design for an image processing Api: a technical report on ITK—the Insight Toolkit. *Stud Health Technol Inform* 2002; 85: 586–592.
28. Dickerson BC, Stoub TR, Shah RC, et al. Alzheimer-signature MRI biomarker predicts AD dementia in cognitively normal adults. *Neurology* 2011; 76: 1395–1402.
29. Yew B and Nation DA. Cerebrovascular resistance: effects on cognitive decline, cortical atrophy, and progression to dementia. *Brain* 2017; 140: 1987–2001.
30. Mattsson N, Tosun D, Insel PS, et al. Association of brain amyloid- $\beta$  with cerebral perfusion and structure in Alzheimer's disease and mild cognitive impairment. *Brain* 2014; 137: 1550–1561.
31. Jagust WJ, Bandy D, Chen K, et al. The Alzheimer's disease Neuroimaging Initiative positron emission tomography core. *Alzheimers Dement* 2010; 6: 221–229.
32. Landau SM, Harvey D, Madison CM, et al. Associations between cognitive, functional, and FDG-PET measures of decline in AD and MCI. *Neurobiol Aging* 2011; 32: 1207–1218.
33. DeCarli C, Miller BL, Swan GE, et al. Predictors of brain morphology for the men of the NHLBI twin study. *Stroke* 1999; 30: 529–536.
34. DeCarli C, Murphy DGM, Teichberg D, et al. Local histogram correction of MRI spatially dependent image pixel intensity nonuniformity. *J Magn Reson Imaging* 1996; 6: 519–528.
35. Fletcher E, Carmichael OT and DeCarli C. MRI non-uniformity correction through interleaved bias estimation and B-spline deformation with a template. *IEEE Eng Med Biol Soc Conf*, <https://ieeexplore.ieee.org/abstract/document/6345882> (2012, accessed 5 December 2019).
36. Scott JA, Braskie MN, Tosun D, et al. Cerebral amyloid and hypertension are independently associated with

- white matter lesions in elderly. *Front Aging Neurosci* 2015; 7: 221.
37. Nation DA, Edland SD, Bondi MW, et al. Pulse pressure is associated with Alzheimer biomarkers in cognitively normal older adults. *Neurology* 2013; 81: 2024–2027.
  38. Qiu C, Winblad B, Viitanen M, et al. Pulse pressure and risk of Alzheimer disease in persons aged 75 years and older. *Stroke* 2003; 34: 594–599.
  39. Hansson O, Seibyl J, Stomrud E, et al. CSF biomarkers of Alzheimer's disease concord with amyloid- $\beta$  PET and predict clinical progression: a study of fully automated immunoassays in BioFINDER and ADNI cohorts. *Alzheimers Dement* 2018; 14: 1470–1481.
  40. Benjamini Y and Hochberg Y. Controlling the false discovery rate: a practical and powerful approach to multiple testing. *J R Stat Soc Ser B Methodol* 1995; 57: 289–300.
  41. Dai W, Lopez OL, Carmichael OT, et al. Mild cognitive impairment and Alzheimer disease: patterns of altered cerebral blood flow at MR imaging. *Radiology* 2009; 250: 856–866.
  42. Fleisher AS, Podraza KM, Bangen KJ, et al. Cerebral perfusion and oxygenation differences in Alzheimer's disease risk. *Neurobiol Aging* 2009; 30: 1737–1748.
  43. Bangen KJ, Restom K, Liu TT, et al. Assessment of Alzheimer's disease risk with functional magnetic resonance imaging: an arterial spin labeling study. *J Alzheimers Dis* 2012; 31: S59–S74.
  44. Hays CC, Zlatar ZZ, Meloy MJ, et al. APOE modifies the interaction of entorhinal cerebral blood flow and cortical thickness on memory function in cognitively normal older adults. *Neuroimage* 2019; 202: 116162.
  45. Zlatar ZZ, Bischoff-Grethe A, Hays CC, et al. Higher brain perfusion may not support memory functions in cognitively normal carriers of the ApoE  $\epsilon$ 4 allele compared to non-carriers. *Front Aging Neurosci* 2016; 8: 151.
  46. Hays CC, Zlatar ZZ, Campbell L, et al. Subjective cognitive decline modifies the relationship between cerebral blood flow and memory function in cognitively normal older adults. *J Int Neuropsychol Soc* 2018; 24: 213–223.
  47. Østergaard L, Aamand R, Gutiérrez-Jiménez E, et al. The capillary dysfunction hypothesis of Alzheimer's disease. *Neurobiol Aging* 2013; 34: 1018–1031.
  48. Iacono D, O'Brien R, Resnick SM, et al. Neuronal hypertrophy in asymptomatic Alzheimer disease. *J Neuropathol Exp Neurol* 2008; 67: 578–589.
  49. Riudavets MA, Iacono D, Resnick SM, et al. Resistance to Alzheimer's pathology is associated with nuclear hypertrophy in neurons. *Neurobiol Aging* 2007; 28: 1484–1492.
  50. Zhang N, Gordon ML and Goldberg TE. Cerebral blood flow measured by arterial spin labeling MRI at resting state in normal aging and Alzheimer's disease. *Neurosci Biobehav Rev* 2017; 72: 168–175.
  51. Bangen KJ, Preis SR, Delano-Wood L, et al. Baseline white matter hyperintensities and hippocampal volume are associated with conversion from normal cognition to mild cognitive impairment in the framingham offspring study. *Alzheimer Dis Assoc Disord* 2018; 32: 50–56.
  52. Brickman AM, Zahodne LB, Guzman VA, et al. Reconsidering harbingers of dementia: progression of parietal lobe white matter hyperintensities predicts Alzheimer's disease incidence. *Neurobiol Aging* 2015; 36: 27–32.